


DOTIL Epigenetically Regulates Autophagy and Mitochondria Fusion in Cell Lines of Renal Cancer

Technology in Cancer Research & Treatment
Volume 22: 1-10
© The Author(s) 2023
Article reuse guidelines:
sagepub.com/journals-permissions
DOI: 10.1177/15330338231167249
journals.sagepub.com/home/tct


Yanguang Hou, MD^{1,2} , Jiachen Liu, MD^{1,2}, Shiyu Huang, MD^{1,2}, Lei Wang, MD¹, Juncheng Hu, PhD^{1,2}, and Xiuheng Liu, MD, PhD¹

Abstract

Objectives: DOTIL, a histone methylase, is overexpression in renal cell cancer. However, the role and detailed molecular mechanism of DOTIL involved in renal cancer development remain unknown. **Methods:** The inhibition of DOTIL was used by SGC0946 and short hairpin RNA silencing. Monodansylcadaverine staining and transmission electron microscope were performed to detect autophagy changes as a result of the inhibition of DOTIL. MitoTracker Red assay was used to analyze mitochondrial morphology. The autophagy markers and mitochondria-related proteins were analyzed by Western blot, qPCR, or immunofluorescence. CHIP assay was performed to demonstrate H3K79me2 is involved in the direct regulation of Farnesoid X receptor transcription. **Results:** DOTIL inhibition increased autophagy activity and promoted mitochondria fusion in cell lines of renal cancer. Inhibition of DOTIL upregulated levels of LC3 α/β , P62, MFN1, and MFN2, which contributed to autophagy activity or mitochondria fusion. DOTIL knockdown showed a similar the above process. DOTIL inhibition or silencing resulted in AMP-activated protein kinase activation and mammalian target of rapamycin inhibition. Mechanistically, the DOTIL inhibitor and its short hairpin RNAs decreased the expression of Farnesoid X receptor in a histone methylase-dependent manner. **Conclusion:** We revealed the essential role of Farnesoid X receptor in regulating DOTIL-induced autophagy and mitochondrial fission through the AMP-activated protein kinase/mammalian target of rapamycin pathway in cell lines of renal cancer, which may provide new insights into the pathogenesis of renal cell cancer.

Keywords

DOTIL, renal cancer, FXR, autophagy, mitochondria fusion

Abbreviations

MDC, Monodansylcadaverine; TEM, transmission electron microscope; AMPK, AMP-activated protein kinase; mTOR, mammalian target of rapamycin; FXR, farnesoid X receptor; CCTCC, China Center for Type Culture Collection; DMSO, dimethyl sulfoxide; CM, conditioned medium; shRNA, short hairpin RNA; RT-qPCR, real-time reverse transcription–quantitative polymerase chain reaction; GAPDH, glyceraldehyde 3-phosphate dehydrogenase; mRNA, messenger RNA; RT, room temperature; IF, immunofluorescence; TCGA, The Cancer Genome Atlas; H3K79, histone 3 lysine 79

Received: September 21, 2022; Revised: February 18, 2023; Accepted: March 13, 2023.

¹ Department of Urology, Renmin Hospital of Wuhan University, Wuhan, Hubei, People's Republic of China

² Wuhan University Institute of Urologic Disease, Renmin Hospital of Wuhan University, Wuhan, Hubei, People's Republic of China

Corresponding Authors:

Juncheng Hu, PhD, Department of Urology, Renmin Hospital of Wuhan University, Wuhan 430060, Hubei, People's Republic of China.

Email: hujc@whu.edu.cn

Xiuheng Liu, MD, PhD, Department of Urology, Renmin Hospital of Wuhan University, Wuhan 430060, Hubei, People's Republic of China.

Email: drliuxh@hotmail.com



Introduction

Histone methylation, defined as a methyl group added to lysine or arginine residues in the histone tail, can alter the chromatin states between histones and DNA, impacting chromatin organization and underlying transcriptional processes.¹ And many of the enzymes responsible for placing (“writers”) and removing (“erasers”) histone methylation has a critical role in tumorigenesis.² Dot1l, the only methyltransferase catalyzing the mono-, di-, and trimethylation of histone 3 lysine 79 (H3K79) (H3K79me2 and -me3), was overexpression in many cancer types, including leukemia,³ prostate cancer,⁴ breast cancer,⁵ and renal cell carcinoma⁶ and was associated with poor clinical outcomes.

Autophagy is a process that delivers cytoplasmic components to lysosomes for degradation. Although the role of autophagy in cancer development and the therapeutic targeting strategies of autophagy in cancer to be sometimes viewed as controversial,⁷ many researchers tried to figure out the connection between histone methylation and autophagy in cancers.^{8–11} EZH2, the methyltransferase catalyzing the di- and trimethylation of H3K27 (H3K27me2 and -me3), inhibits autophagosome formation in HeLa cells.^{11,12} Knockdown or inhibition of G9a, the methyltransferase of H3K9 induced the activation of autophagy in glioblastoma.¹³

A previous study found that DOT1L-regulated, H3K79me2-mediated, increases autophagy activity, and protects against osteoporosis.¹⁴ Moreover, DOT1L inhibitor (SGC0946) enhanced the selective autophagic degradation by downregulating lysosome-associated membrane protein LAMP5 in MLL leukemia and linking H3K79 methylation to autophagy regulation.¹⁵ But it is not clear whether DOT1L could regulate autophagy in renal cell carcinoma.

In this study, we found that DOT1L inhibition or silencing increases autophagy activity and promotes mitochondria fusion in cell lines of renal cancer by upregulating the AMP-activated protein kinase (AMPK)–mammalian target of rapamycin (mTOR) signaling axis. We demonstrated that DOT1L exerted this effect by epigenetically activating Farnesoid X receptor (FXR) transcription, which suggests a potential therapeutic implication in the management of renal cell carcinoma.

Materials and Methods

General Reagents and Antibodies

SGC0946 (#HY-15650, HPLC \geq 99.68%), FXR inhibitor Guggulsterone (HY-107738), and agonist INT767 (HY-12434) were purchased from MedChemExpress. Lipo293tm Transfection Reagent (#C0521) and Blasticidin (#ST018-10 mg) were from Beyotime Biotechnology. DOT1L (#ab239358), H3K79me2 (#ab3594), H3K79me3 (#ab8898), MFN1 (Mitofusin 1) (ab221661), and MFN2 (Mitofusin 2) (ab205236) antibodies were from Abcam. P62/SQSTM1 (#88588), LC3 α/β Antibody (#4108), AMPK α (D5A2) (#583), Phospho-AMPK α (Thr172) (#2535), mTOR (#2972), and FXR/NR1H4 (#72105) were

purchased from Cell Signaling Technology. GAPDH (#10494-1-AP) and H3 (#17168-1-AP) were from Proteintech Group.

Cell Culture and Treatments

Renal cancer cell lines 786-O(GDC0159) and 769P(GDC0103) were purchased from China Center for Type Culture Collection and grown as recommended in RPMI-1640 containing 10% FBS at 37 °C in 5% CO₂. HEK 293 T(GDC0187) was grown in DMEM (Biosharp: BL301A) culture medium containing 10% FBS. SGC0946 was dissolved in dimethyl sulfoxide (DMSO) as 10 mM stock solutions. The working concentration is 0 (DMSO), 5, and 10 μ M, respectively. Guggulsterone and INT767 were the same dissolved in DMSO. The working concentration of Guggulsterone is 20 μ M and INT767 is 10 μ M, respectively.

Plasmids and Lentivirus

For short hairpin RNA (shRNA)-mediated Dot1L gene knock-down, 2 shRNAs were cloned in pLKO.1 lentiviral vector with Age I and EcoR I enzymatic restriction sites. The oligos of shRNAs were synthesized in Sangon Biotech. The sequences of shRNAs are listed in Supplemental Table 1. pLKO.1, psPAX2, and pMD2.G (Addgene), the 3 plasmids were cotransfected into HEK 293T, and the conditioned medium (CM) was collected after 48 h and 72 h. Ctrl, the shRNA not targeting any known gene, was used as control group. Then, the CM was added to 786-O cells. The cells with stable transfection were selected with Blasticidin.

Real-Time Quantitative Polymerase Chain Reaction

Total RNA was isolated using Trizol (Invitrogen). RT-PCR analysis was carried out in a CFX96 TouchTM Real-Time PCR Detection system (Bio-Rad Laboratories, Inc) or a Roche LightCycler 480-II system. PrimeScript RT reagent Kit with gDNA Eraser (Cat. #RR047A) is a reverse-transcription kit for real-time reverse transcription–quantitative polymerase chain reaction (RT-qPCR) that includes a genomic DNA elimination reaction, and the combination with quantitative PCR reagent such as TB Green®Premix Ex TaqTM II (Tli RNaseH Plus) (Cat. #RR820A). The primer sequences used for PCR are shown in Supplemental Table 2. The relative messenger RNA (mRNA expression) levels were normalized to that of glyceraldehyde 3-phosphate dehydrogenase (GAPDH).

Western Blot Analysis

We used ice-cold RIPA lysis buffer lysed and harvested cells. After centrifugation at 12 000 \times g for 15 min at 4 °C, the proteins in the supernatants were quantified by Bradford method and separated using suitable concentration SDS-PAGE gel and electro-transferred from the gel to a PVDF membrane (Merck & Co). Following blocking with 5% skimmed milk in phosphate-

buffered saline, we put the membranes and the primary antibodies together at 4 °C overnight. Then the membranes were immunoblotted by specifically bound HRP (Biosharp: BL003A)-conjugated secondary antibodies and detected by an ECL detection system (ChemiDoc™ XRS + machine, Bio-Rad). Protein levels of GAPDH and H3 were employed as loading controls.

Monodansylcadaverine Staining

Monodansylcadaverine (MDC) staining was performed by Autophagy Staining Assay Kit with MDC (#C3018S, Bryotime), which is a rapid and convenient kit for detecting autophagy by using dansylcadaverine, also known as MDC as a fluorescent probe. In detail, treated cells were stained with MDC for 40 min at 37 °C and then detected by fluorescence microscope (BX53, OLYMPUS).

Immunofluorescence

After treatment, cell climbing sheets were fixed in 4% paraformaldehyde for 20 min at room temperature (RT). After washing with PBS (Servicebio: G4202), to permeabilize cell membranes, the cells were treated with 200 μ L 1% Triton-X 100 for 5 min on shaking table at RT. Then, block with 10% goat serum for 1 h and incubated with anti-P62, anti-LC3 α/β for 2 h at RT. Subsequently, the cells were incubated with fluorescent-conjugated secondary antibodies against rabbit (Alexa Fluor 488, Thermo) for 1 h at RT and protected from light. DAPI (Beyotime) was used to stain and evaluate nuclear morphology.

MitoTracker Red Assay

After treatment, a 100 nM MitoTracker Red CMXRos (C1049B-50 μ g, Beyotime) working solution was prepared for staining. 786-O cells with MitoTracker Red dye were incubated for 30 min at 37 °C. After incubation, the cells were washed 3 times with prewarmed PBS. Finally, the cells were observed under oil and fluorescence microscope. Mitochondrial morphology was analyzed by Image J (v1.52v) with a MINA plugin.

Transmission Electron Microscope

To detect autophagy in 786-O cells, transmission electron microscope (TEM) analysis was performed. The 786-O cells were fixed in 2.5% glutaraldehyde overnight and subsequently fixed in 1% osmium tetroxide for 1 h. After samples underwent gradient ethanol dehydration, the cells were embedded. Finally, the ARPE-19 cell morphology was observed under a TEM (JEOL Ltd).

ChIP Assay

ChIP assays were performed following the protocols as Kit description (ChIP Assay Kit(P2078), Beyotime Biotechnology). In brief, crosslinking was performed with 1% formaldehyde at

RT for 10 min, and the reaction was stopped by treatment with 0.125 M glycine. The cell pellets were resuspended in 200 mL of SDS lysis buffer and sonicated using a Bioruptor. The cell lysates were then immunoprecipitated with H3K79me2 antibodies overnight at 4 °C and further incubated with salmon sperm DNA coupled to protein A-agarose (Millipore) for 2 h at 4 °C. The precipitates were washed, eluted, and then reverse-crosslinked with 20 mL 5 M NaCl by incubating at 65 °C 4 h. DNA fragments were precipitated from the eluate and dissolved in ddH₂O. We designed 5 pairs of primers of different location in FXR promoter (Supplemental Table 3). And then PCR was performed with the PrimeSTAR[®] Max DNA Polymerase (#R045A, TAKARA).

Statistical Analyses

Statistical analyses were performed using unpaired 2-tailed Student *t* test. Survival studies were analyzed by Log-rank (Mantel-Cox) test. Correlations were analyzed by Spearman correlation coefficient (*r*). Data are presented as mean \pm standard error of the mean, unless otherwise indicated. For all analyses, results were considered statistically significant with *P* < .05, **P* < .05, ***P* < .01, and ****P* < .001.

Results

DOT1L Inhibition Leads to Autophagy Increased in Renal Cell Cancer Cells

After treatment with SGC0946 for 24 h, H3K79me2 and H3K79me3 were both decreased in cell lines of renal cancer (Figure 1A and Supplemental Figure 1A). To confirm that autophagy is involved in the effects of SGC0946 in renal cell cancer, we found that SGC0946 treatment significantly increased the expression level of LC3 α/β ratio, and p62/SQSTM1, 2 markers of autophagy, in cell lines of renal cancer (Figure 1B and Supplemental Figure 1B and C). Then the MDC staining for autophagosome detection was conducted. As illustrated in Figure 1C and D, the MDC-stained puncta in 786-O cells significantly increased in the SGC0946-treated group. The number of autophagosomes was positive correlations with SGC0946 concentration. Transmission electron microscopy confirmed that SGC0946 treatment increased the number of autophagy-associated vesicles (Figure 1E and F). We used immunofluorescence to stain LC3 α/β , to detect autophagy in renal cancer after treatment with SGC0946. The result showed that SGC0946 enforced the expression of LC3 in the cytoplasm (Figure 1G and H). Collectively, these data suggest that SGC0946, the DOT1L inhibitor, activates autophagy in renal cancer cells.

DOT1L Inhibition Leads to Abnormal Mitochondrial Dynamics in Cell Lines of Renal Cancer

Accumulative evidence suggests that mitochondria fission and fusion machinery, as well as a number of components, including dynamin-related protein 1 (Drp1), mitofusin 1 and 2 (MFN1 and MFN2), are related to apoptosis and

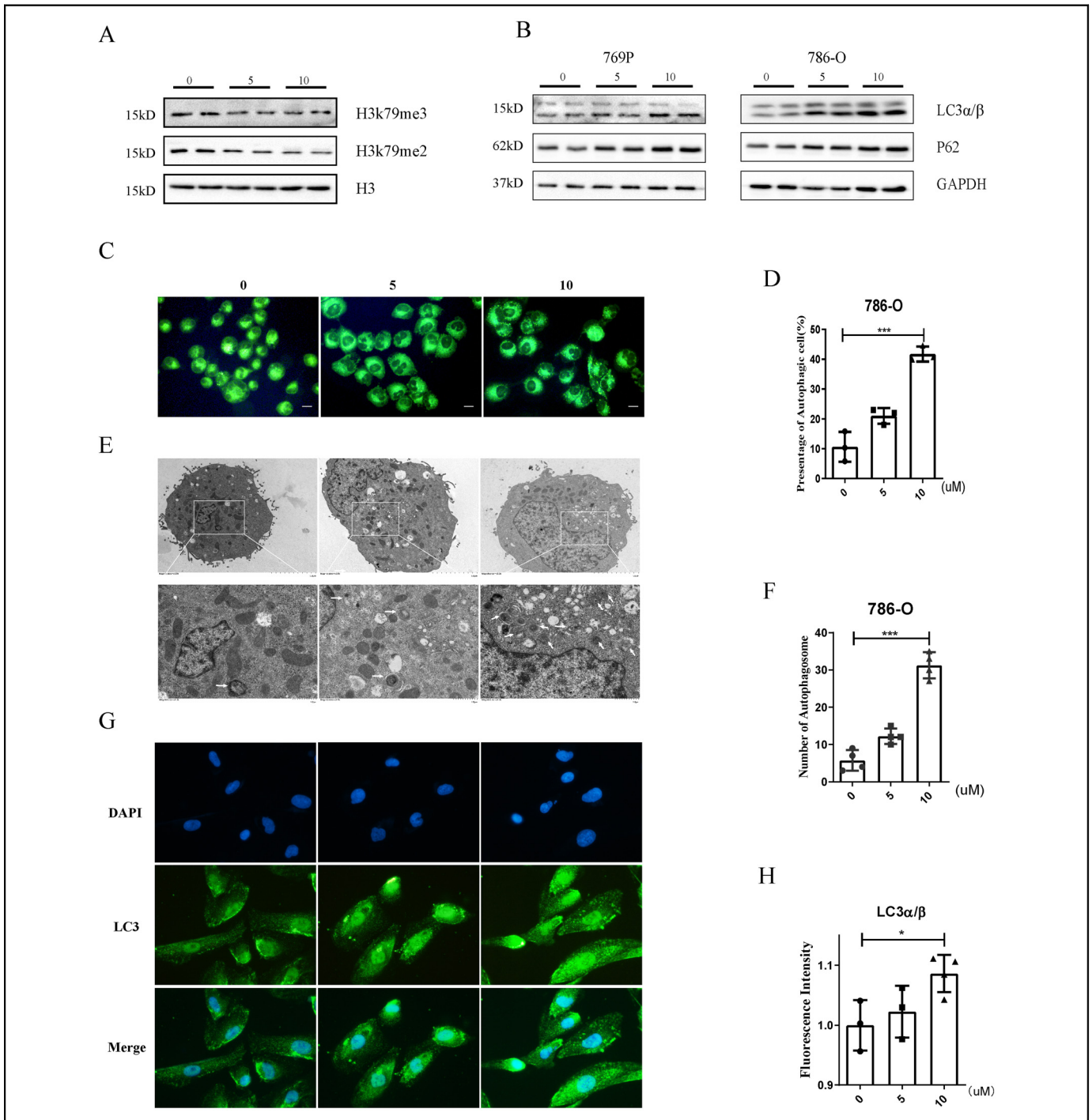


Figure 1. SGC0946 leads to autophagy increased in renal cell cancer cells. (A) 786-O cells were treated with SGC0946 (0, 5, and 10 μ M) for 24 h. Western blot showed H3K79me2 in 786-O cells. (B) The LC3 α/β and p62 expression were determined by Western blot after treatment with SGC0946 at different concentration for 24 h. (C and D) Monodansylcadaverine (MDC) staining was used to detect the autophagy of 786-O cells. The cells were treated with SGC0946 (0, 5, and 10 μ M) for 24 h and analyzed by confocal microscope. Statistics of relative puncta are shown in the right histogram. Scar bar = 20 μ m. (E and F) Representative images of transmission electron microscopy (TEM). The white arrows indicate autophagosomes. $***P < .001$, compared with 0 μ M group. (Up 3.0 k magnification; Down 8.0 k magnification). (G and H) Immunofluorescence staining was performed to detect the p62 and LC3 α/β expression in 786-O cells (560 \times magnification).

autophagy.^{16,17} We further evaluated mitochondrial fission and fusion in cell lines of renal cancer after SGC0946 treatment. MitoTracker Red CMXRos probe was stained to

indicate the morphology of mitochondria, and the results suggested mitochondria were fused after SGC0946 treatment (Figure 2A). We then quantified changes in mitochondrial

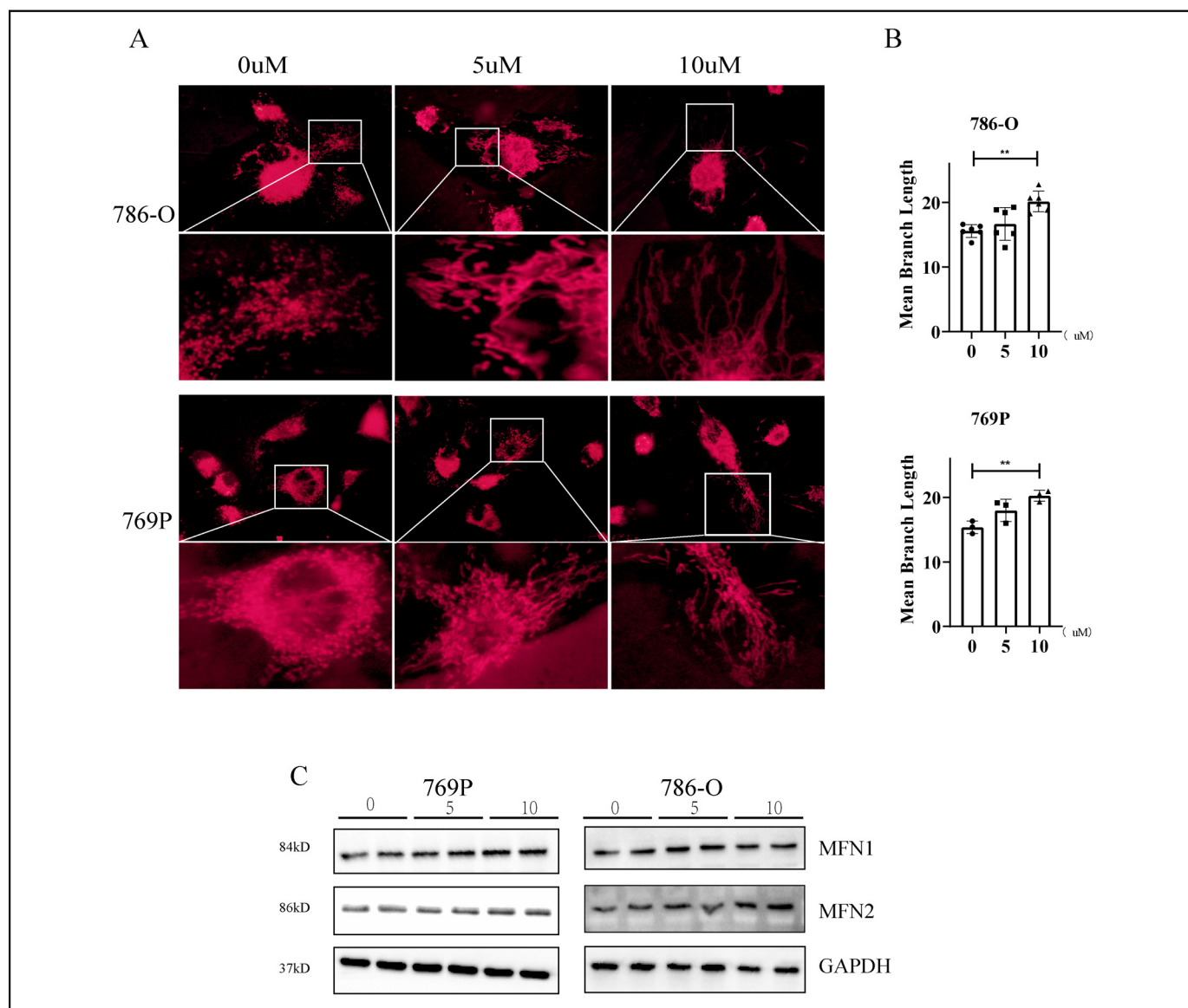


Figure 2. DOT1L inhibition leads to abnormal mitochondrial dynamics in cell lines of renal cancer. (A) Representative picture of 786-O and 769P cells stained with Mito-Tracker Red CMXRos, captured using oil-Fluorescence microscope, which shows the morphology of mitochondria in each group (up, scale bar = 10 μ m). (B) Data showing the mean branch length of mitochondrial in each group measured by Image J analysis. $**P < .01$ compared with 0 μ M group. (C) Representative immunoblots showing SGC0946 increased the protein expression of Mitofusin 1 (MFN1) and Mitofusin 2 (MFN2) in SGC0946-treated 786-O cells.

morphology by MINA plugin in Image J. Compared with 0 μ M group, the mean branch length of mitochondrial was increased 5 μ M and 10 μ M group (Figure 2B). Additionally, the Western blot results showed that SGC0946 treatment significantly promoted MFN1 and MFN2 protein expression in cell lines of renal cancer (Figure 2C and Supplemental Figure 2A and B).

DOT1L Silencing Leads to Autophagy Increased in Renal Cell Cancer Cells

To further elucidate the function of DOT1L in renal cells, we silenced DOT1L in 786-O and 769P cells by using 2

lentivirus-mediated shRNAs. DOT1L was successfully knockdown by shRNA lentiviral particles and the results were verified by RT-PCR (Figure 3A) and Western blot (Figure 3B and Supplemental Figure 3A). And meanwhile the level of H3K79me2 and H3K79me3 was reduced responding to knockdown of DOT1L (Figure 3B and Supplemental Figure 3B). Then we perform the MDC staining for autophagosomes detection in DOT1L knockdown 786-O cells. As illustrated in Figure 3C, the number of autophagic cells in DOT1L knockdown group significantly increased compared to the control (ctrl) group. Then we found that the protein level of LC3 α / β ratio, and p62/SQSTM1 significantly increased in DOT1L knockdown

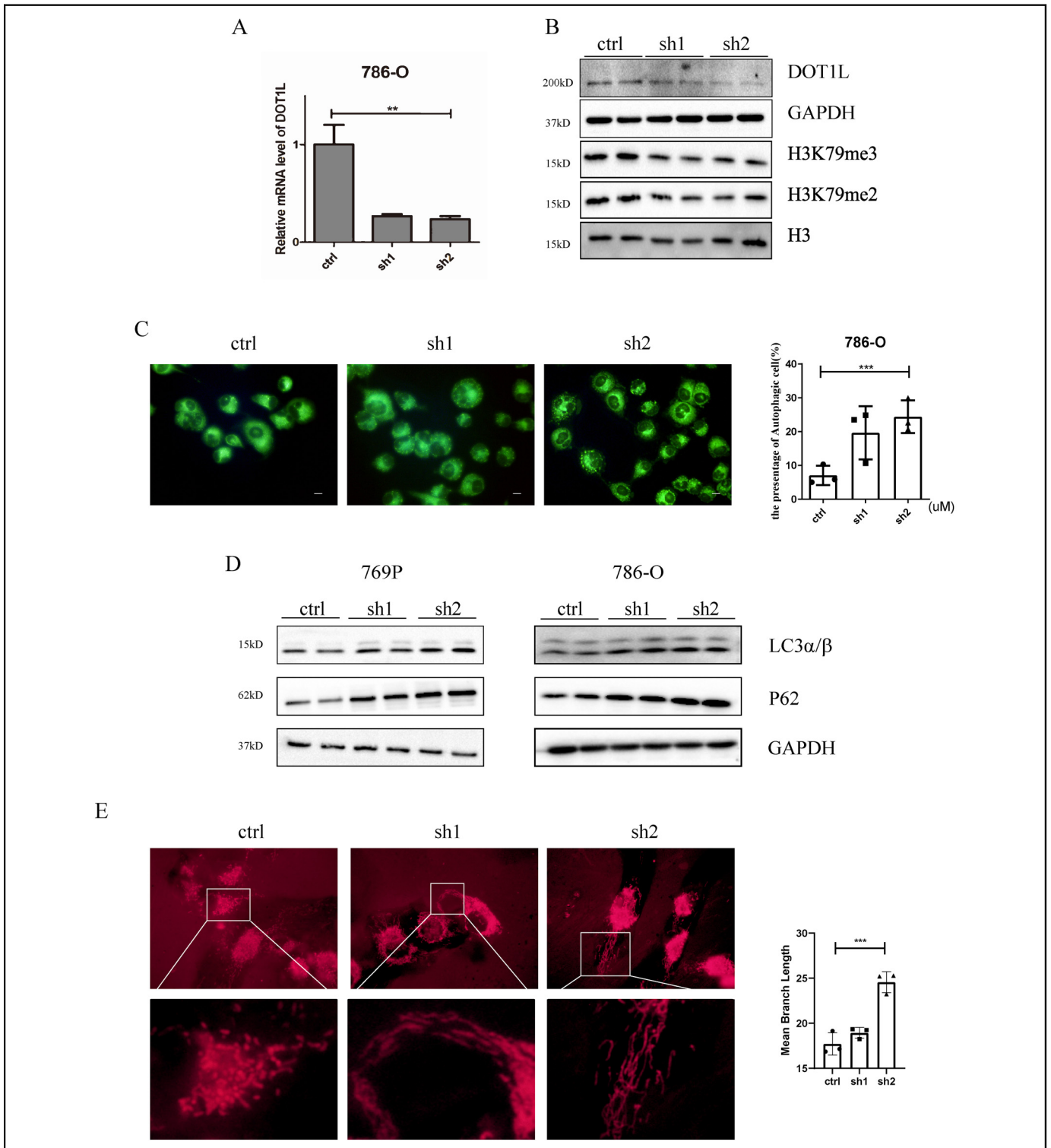


Figure 3. DOT1L knockdown leads to autophagy increased in renal cancer. (A) Relative messenger RNA (mRNA) expression of DOT1L detected by using qRT-PCR in 786-O renal cancer cell lines after DOT1L knockdown. (B) Protein expression of DOT1L, H3K79me2, and H3K79me3 detected by Western blot in 786-O cells after DOT1L knockdown. (C) Monodansylcadaverine (MDC) staining was used to detect the autophagy of 786-O cells after DOT1L knockdown. Statistics of relative puncta are shown in the right histogram. Scar bar = 20 μ m. (D) The LC3 α/β and p62 expression were determined by Western blot in 786-O cells and 769P cells after DOT1L knockdown. (E) Representative pictures of 786-O cells contained with MitoTracker Red CMXRos, captured using oil-fluorescence microscope, which shows the morphology of mitochondria in control, sh1 and sh2 group (up, scale bar = 10 μ m). *** $P < .001$, compared with ctrl group.

786-O cells (Figure 3D). Together, these data suggest that DOT1L knockdown promotes autophagy in the renal cancer cells. Then we evaluated mitochondrial morphology after DOT1L knockdown, and the results showed mitochondria were fused (Figure 3E).

DOT1L Inhibition or Silencing Induces Autophagy by Activating the AMPK/mTOR Signaling Pathway in Cell Lines of Renal Cancer

To seek out potential DOT1L-related autophagy pathways, the public data of KIRC were downloaded from The Cancer

Genome Atlas (TCGA) and GSEA was applied. According to GSEA, we identified 15 KEGG signaling pathways that showed significantly different enrichment in the DOT1L expression phenotype (Figure 4A), and in which mTOR signaling pathway was closely related to autophagy (Figure 4B). As shown in Figure 4C and D, SGC0946 significantly enhanced the phosphorylation and total of AMPK and reduced total levels of mTOR. And similarly, DOT1L knockdown significantly enhanced the phosphorylation and total of AMPK and reduced total levels of mTOR (Figure 4E and F). All the results revealed that DOT1L inhibition or silencing regulated autophagy by activating the AMPK/mTOR signaling pathway in cell lines of renal cancer.

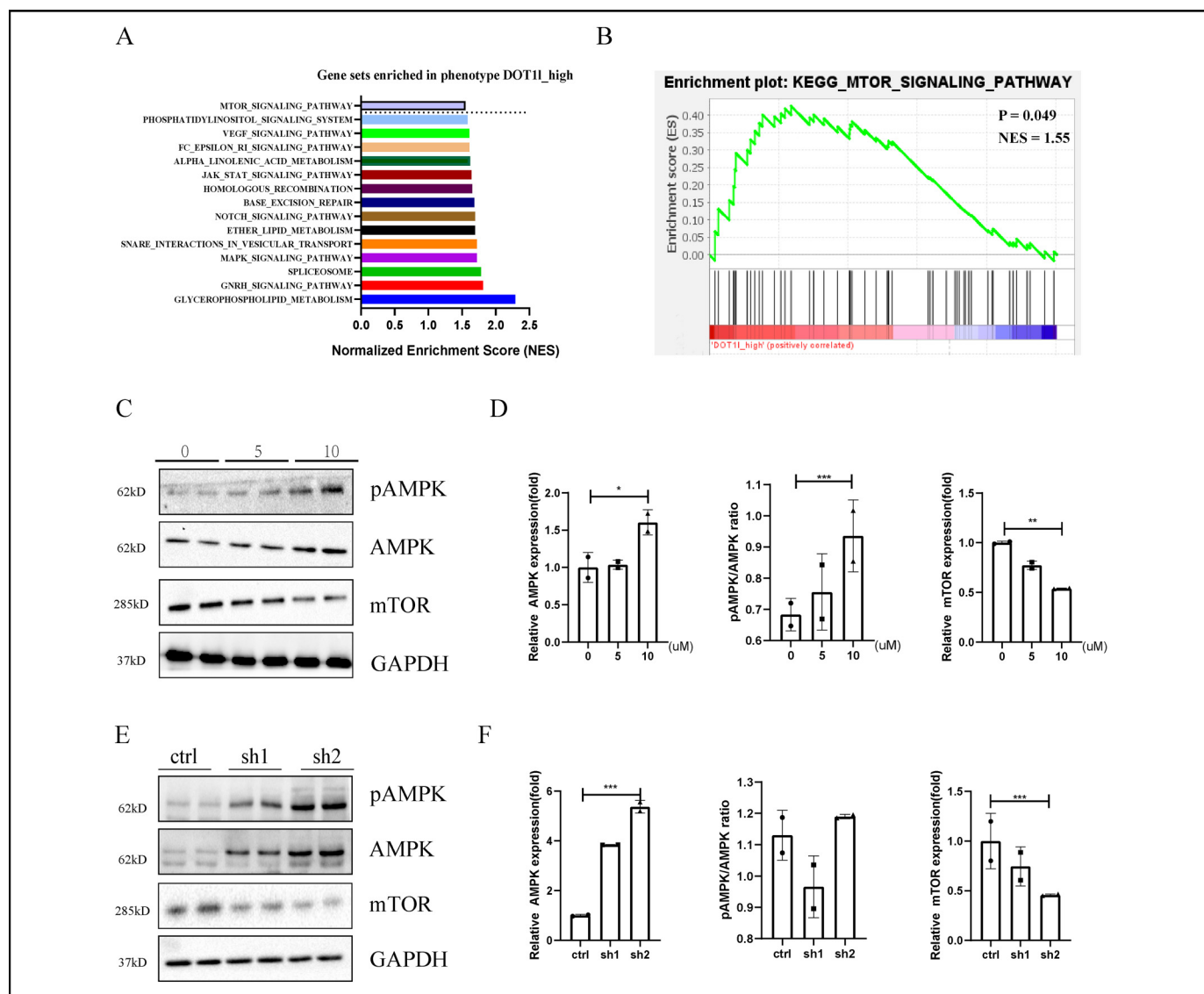


Figure 4. DOT1L inhibition or silencing induces autophagy by activating the AMP-activated protein kinase (AMPK)/mammalian target of rapamycin (mTOR) signaling pathway. (A) Gene sets enriched 15 KEGG signaling pathways in phenotype DOT1L_high. (B) GSEA indicated that DOT1L expression was closely related to mTOR signaling in renal cancer samples (TCGA-KIRC). (C and D) Western blot analysis showing the total and phosphorylated levels of AMPK, mTOR in SGC0946 treated renal cancer cells. (E and F) Western blot analysis showing the total and phosphorylated levels of AMPK, mTOR in DOT1L knockdown renal cancer cells. * $P < .05$, ** $P < .01$, and *** $P < .001$, compared with ctrl group.

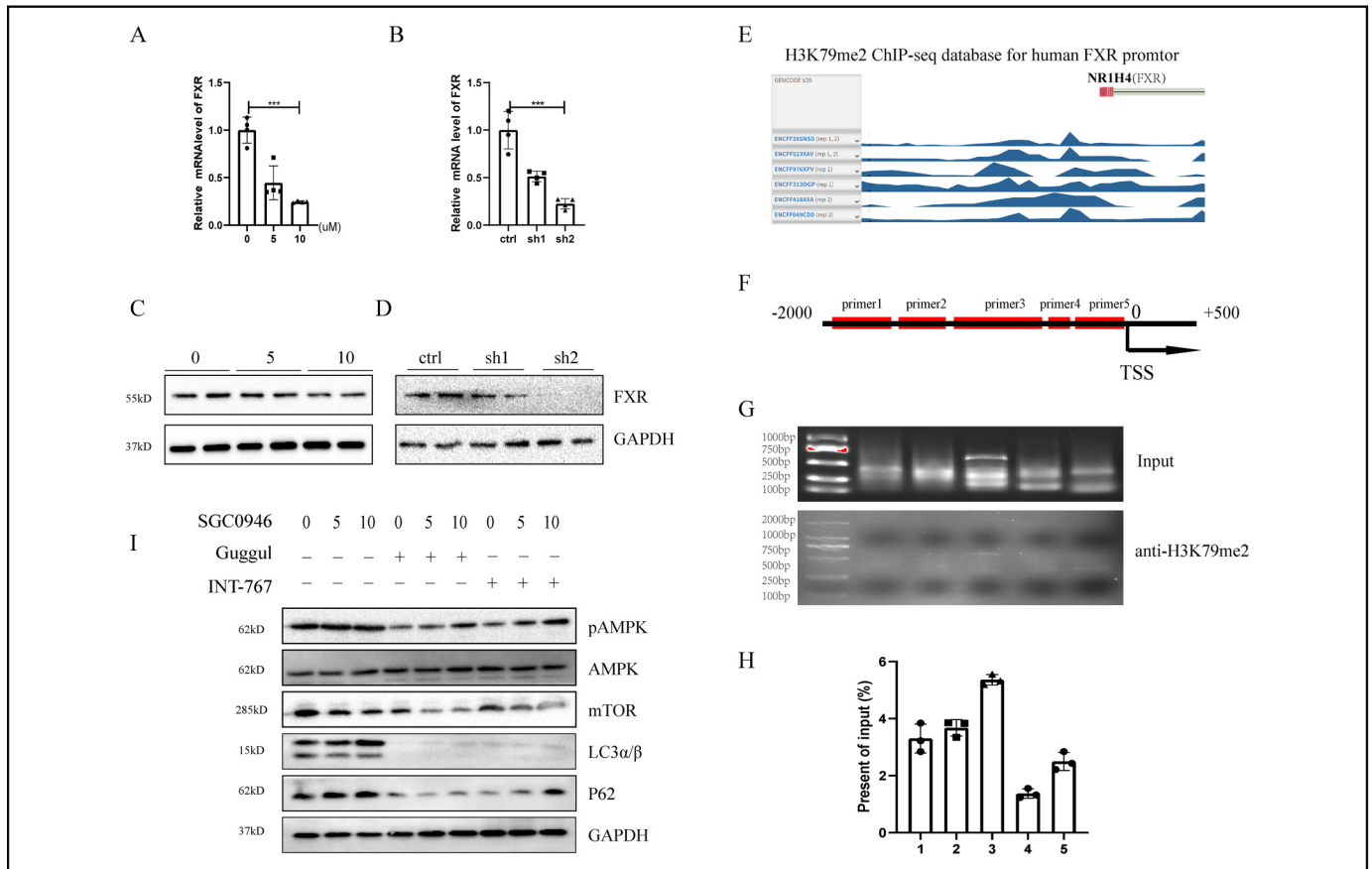


Figure 5. DOT1L activated AMP-activated protein kinase (AMPK)/mammalian target of rapamycin (mTOR) signaling pathway by direct regulation of Farnesoid X receptor (FXR). (A and B) qPCR was performed to detect FXR expression levels in SGC0946 treatment 786-O cells or DOT1L knockdown 786-O cells. (C and D) The protein levels of FXR were detected by Western blot in SGC0946 treatment 786-O cells or DOT1L knockdown 786-O cells. (E) H3K79me2 ChIP-seq in ENCODE database showing FXR promoter in humans. (F) Schematic diagram showed the location of 5 pairs of primers in FXR promoter regions. (G) ChIP assays were performed using H3K79me2 antibody in 786-O cells to detect the binding sites in FXR promoter regions. (H) ChIP-qPCR assays were performed using H3K79me2 antibody in 786-O cells. The normalized expression in 786-O cells was input. (I) 786-O cells were treated with SGC0946, then treated with Guggulsterone (20 μM) or INT767 (10 μM) for 24 h and harvested for Western blot.

DOT1L Inhibition or Silencing Activated AMPK/mTOR Signaling Pathway by Regulation of FXR in Cell Lines of Renal Cancer

Recently, FXR (also known as NR1H4), the bile acid receptor, is a member of the nuclear receptor superfamily and has been implicated in the regulation of autophagy¹⁸ and mitochondrial morphology.^{19,20}

We first observed the mitochondrial morphology after different treatment of FXR in 786-O cells. The result showed that FXR agonist INT-767 inhibited mitochondria fusion and decreased MFN2 protein expression in 786-O cells. And the reverse result is observed after treatment with FXR inhibitor Guggulsterone (Supplemental Figure 4A and B).

A previous study found FXR/AMPK signaling pathway had a critical role in acute liver injury.²¹ We hypothesize that DOT1L might activate autophagy through the FXR/AMPK signaling pathway in cell lines of renal cancer. First, we analyzed and

established a positive correlation between DOT1L and FXR mRNA expression in renal cancer tissues through the TCGA database (Supplemental Figure 5A). Next, to validate their correlation, we performed the IHC assay to detect the protein levels of DOT1L and FXR in human renal specimens. Our results showed that samples with higher DOT1L expression were frequently associated with higher FXR level (Supplemental Figure 5B). DOT1L inhibition or silencing significantly decreased the mRNA and protein levels of FXR (Figure 5A-D and Supplemental Figure 5C and D). H3K79me2 is an active gene mark in mammalian cells and occurs on the promoter and 5' regions within the coding regions of transcriptionally active genes. ChIP-seq data revealed high H3K79me2 occupancies in the key regulatory regions of the FXR promoter in human (Figure 5E). ChIP assay demonstrated a high H3K79me2 abundance binding to the FXR promoter (Figure 5F-H). Thus, H3K79me2 is involved in the direct regulation of FXR transcription in cell lines of renal cancer.

Next, we treated 786-O cells with SGC0946 and FXR inhibitors or agonists, followed by Western blot. SGC0946 treatment in combination with Guggulsterone significantly reduced pAMPK protein level and upregulated mTOR level (Figure 5I). SGC0946 treatment with INT-767 increased pAMPK protein level and downregulated mTOR level. Meanwhile, the protein level of LC3 α/β and p62 in SGC0946 and INT-767 group was higher than SGC0946 and Guggulsterone group (Figure 5I and Supplemental Figure 5C). Together, these results demonstrate that DOT1L promoted autophagy by induced FXR expression in cell lines of renal cancer.

Discussion

Autophagy is a process that cellular unnecessary or dysfunctional components are transported to lysosomes for degradation. In recent years, emerging evidence suggests that histone methylation plays an important role in autophagy regulation.^{22,23} SQSTM1/p62 transcription and autophagy activity are both inhibited by WNT/-catenin signal activation, which is connected to the rise of H3K4me3 levels.²⁴ EZH2 depletion or inhibition reduced H3K27me3 and activated autophagy in non-small cell lung cancer cells and rectal colon cancer cells, indicating that EZH2 is a negative regulator of autophagy.^{25,26} A previous study found DOT1L inhibition (EPZ5676) increases autophagy flux and migration ability of 40-h pre-Osteoclasts.¹⁴ In our study, we found DOT1L inhibition (SGC0946) or knock-down activated autophagy in cell lines of renal cancer.

In this study, we demonstrate that DOT1L regulates mTOR signaling pathway, suggesting a possible link between the mTOR signaling pathway and epigenetic regulation. Autophagy is one of the major biological processes regulated by the mTOR signaling pathway. The mTOR pathway is a clinically relevant target in renal cancer due to its frequently hyper-activated in ccRCC.^{27,28} Everolimus and Temsirolimus, 2 mTOR inhibitors, are licensed for clinical use in ccRCC patients.^{29,30} Therefore, our study may open up the possibility that SGC0946 may be a potential target for cancer treatment.

Mitochondrial morphology is in dynamic equilibrium within cells and mitochondrial fission and fusion. Cellular stress and exposure to toxicant may result in mitochondrial fusion or fission.³¹ Our results demonstrated that treatment with SGC0946 and DOT1L knockdown increased mitochondrial fusion in cell lines of renal cancer.

FXR is a nuclear transcription factor and highly expressed in liver,³² kidney,³³ and heart.³⁴ Previous reports have suggested that FXR is closely related to autophagy. FXR activation reduced the expression of pS6, a marker of mTORC1 activation.^{35,36} Our previous study found that knockdown of NRIH4 significantly suppressed cancer cell proliferation, migration, and invasion.³⁷ In this study, we demonstrated that DOT1L acts as a histone methyltransferase to transactivate the FXR promoter in cell lines of renal cancer. And DOT1L regulated autophagy by mediating FXR expression.

However, one limitation of this study is that of standard cell culture techniques since they do not mimic physiological

conditions, lacking *in vivo* part. Thus, additional *in vivo* studies will be needed to further determine the significance of our results.

Conclusion

We described the role of the DOT1L-FXR axis in cell lines of renal cancer. DOT1L regulated autophagy of renal cancer cells via H3K79 methylation enrichment at the FXR promoter, which may provide new insights into the pathogenesis of renal cell cancer.

Authors' Contribution

Yanguang Hou, Jiachen Liu, and Shiyu Huang contributed equally to this work.


Declaration of Conflicting Interests

The author(s) declared no potential conflicts of interest with respect to the research, authorship, and/or publication of this article.

Funding Statement

The author(s) disclosed receipt of the following financial support for the research, authorship, and/or publication of this article: This research was supported by grants from National Natural Science Foundation of China (No. 81972408), the key research and development program of Hubei Province (No. 2020BCB051), and the Fundamental Research Funds for the Central Universities (2042021kf0105).

ORCID iD

Yanguang Hou  <https://orcid.org/0000-0003-1258-8449>

Supplemental Material

Supplemental material for this article is available online.

References

1. Black JC, Van Rechem C, Whetstine JR. Histone lysine methylation dynamics: establishment, regulation, and biological impact. *Mol Cell*. 2012;48(4):491-507.
2. Hyun K, Jeon J, Park K, Kim J. Writing, erasing and reading histone lysine methylations. *Exp Mol Med*. 2017;49(4):e324.
3. Sarno F, Nebbioso A, Altucci L. DOT1L: a key target in normal chromatin remodelling and in mixed-lineage leukaemia treatment. *Epigenetics*. 2020;15(5):439-453.
4. Vatapalli R, Sagar V, Rodriguez Y, et al. Histone methyltransferase DOT1L coordinates AR and MYC stability in prostate cancer. *Nat Commun*. 2020;11(1):4153.
5. Cho MH, Park JH, Choi HJ, et al. DOT1L cooperates with the c-Myc-p300 complex to epigenetically derepress CDH1 transcription factors in breast cancer progression. *Nat Commun*. 2015;6:1-14.
6. Qu Y, Liu L, Wang JJ, et al. Dot1 l expression predicts adverse postoperative prognosis of patients with clear-cell renal cell carcinoma. *Oncotarget*. 2016;7(51):84775-84784.
7. Levy JMM, Towers CG, Thorburn A. Targeting autophagy in cancer. *Nat Rev Cancer*. 2017;17(9):528-542.

8. Artal-Martinez de Narvajias A, Gomez TS, Zhang JS, et al. Epigenetic regulation of autophagy by the methyltransferase G9a. *Mol Cell Biol.* 2013;33(20):3983-3993.
9. Shen B, Tan M, Mu X, et al. Upregulated SMYD3 promotes bladder cancer progression by targeting BCLAF1 and activating autophagy. *Tumour Biol.* 2016;37(6):7371-7381.
10. Shin HJ, Kim H, Oh S, et al. AMPK-SKP2-CARM1 signalling cascade in transcriptional regulation of autophagy. *Nature.* 2016;534(7608):553-557.
11. Wei FZ, Cao ZY, Wang X, et al. Epigenetic regulation of autophagy by the methyltransferase EZH2 through an MTOR-dependent pathway. *Autophagy.* 2015;11(12):2309-2322.
12. Li R, Yi X, Wei X, et al. EZH2 inhibits autophagic cell death of aortic vascular smooth muscle cells to affect aortic dissection. *Cell Death Dis.* 2018;9(2):1-15.
13. Ke XX, Zhang R, Zhong X, Zhang L, Cui H. Deficiency of G9a inhibits cell proliferation and activates autophagy via transcriptionally regulating c-Myc expression in glioblastoma. *Front Cell Dev Biol.* 2020;8:593964.
14. Gao Y, Ge W. The histone methyltransferase DOT1L inhibits osteoclastogenesis and protects against osteoporosis. *Cell Death Dis.* 2018;9(2):33.
15. Wang WT, Han C, Sun YM, et al. Activation of the lysosome-associated membrane protein LAMP5 by DOT1L serves as a bodyguard for MLL fusion oncoproteins to evade degradation in leukemia. *Clin Cancer Res.* 2019;25(9):2795-2808.
16. Abate M, Festa A, Falco M, et al. Mitochondria as playmakers of apoptosis, autophagy and senescence. *Semin Cell Dev Biol.* 2020;98:139-153.
17. Otera H, Miyata N, Kuge O, Mihara K. Drp1-dependent mitochondrial fission via MiD49/51 is essential for apoptotic cristae remodeling. *J Cell Biol.* 2016;212(5):531-544.
18. Panzitt K, Fickert P, Wagner M. Regulation of autophagy by bile acids and in cholestasis—CholestoPHAGY or CholeSTOPAgY. *Biochim Biophys Acta Mol Basis Dis.* 2021;1867(2):166017.
19. Comeglio P, Cellai I, Mello T, et al. INT-767 prevents NASH and promotes visceral fat brown adipogenesis and mitochondrial function. *J Endocrinol.* 2018;238(2):107-127.
20. Han CY, Kim TH, Koo JH, Kim SG. Farnesoid X receptor as a regulator of fuel consumption and mitochondrial function. *Arch Pharm Res.* 2016;39(8):1062-1074.
21. Zheng LL, Yin LH, Xu LN, et al. Protective effect of dioscin against thioacetamide-induced acute liver injury via FXR/AMPK signaling pathway in vivo. *Biomed Pharmacother.* 2018;97:481-488.
22. Baek SH, Kim KI. Epigenetic control of autophagy: nuclear events gain more attention. *Mol Cell.* 2017;65(5):781-785.
23. Hu LF. Epigenetic regulation of autophagy. *Autophagy Biol Dis Basic Sci.* 2019;1206:221-236.
24. Petherick KJ, Williams AC, Lane JD, et al. Autolysosomal beta-catenin degradation regulates Wnt-autophagy-p62 crosstalk. *EMBO J.* 2013;32(13):1903-1916.
25. Wei FZ, Cao Z, Wang X, et al. Epigenetic regulation of autophagy by the methyltransferase EZH2 through an MTOR-dependent pathway. *Autophagy.* 2015;11(12):2309-2322.
26. Cao P, Li Y, Shi R, et al. Combining EGFR-TKI with SAHA overcomes EGFR-TKI-acquired resistance by reducing the protective autophagy in non-small cell lung cancer. *Front Chem.* 2022;10:837987.
27. Pantuck AJ, Seligson DB, Klatte T, et al. Prognostic relevance of the mTOR pathway in renal cell carcinoma: Implications for molecular patient selection for targeted therapy. *Cancer.* 2007;109(11):2257-2267.
28. Robb VA, Karbowniczek M, Klein-Szanto AJ, Henske EP. Activation of the mTOR signaling pathway in renal clear cell carcinoma. *J Urol.* 2007;177(1):346-352.
29. Hudes G, Carducci M, Tomczak P, et al. Temsirolimus, interferon alfa, or both for advanced renal-cell carcinoma. *N Engl J Med.* 2007;356(22):2271-2281.
30. Motzer RJ, Escudier B, Oudard S, et al. Efficacy of everolimus in advanced renal cell carcinoma: a double-blind, randomised, placebo-controlled phase III trial. *Lancet.* 2008;372(9637):449-456.
31. Meyer JN, Leuthner TC, Luz AL. Mitochondrial fusion, fission, and mitochondrial toxicity. *Toxicology.* 2017;391:42-53.
32. Kim SG, Kim BK, Kim K, Fang S. Bile acid nuclear receptor farnesoid X receptor: therapeutic target for nonalcoholic fatty liver disease. *Endocrinol Metab (Seoul).* 2016;31(4):500-504.
33. Marquardt A, Al-Dabet MM, Ghosh S, et al. Farnesoid X receptor agonism protects against diabetic tubulopathy: potential add-on therapy for diabetic nephropathy. *J Am Soc Nephrol.* 2017;28(11):3182-3189.
34. Gao JS, Liu XQ, Wang BJ, et al. Farnesoid X receptor deletion improves cardiac function, structure and remodeling following myocardial infarction in mice (vol 16, pg 673, 2017). *Mol Med Rep.* 2017;16(6):9270-9270.
35. Jung K, Kim M, So J, Lee SH, Ko S, Shin D. Farnesoid X receptor activation impairs liver progenitor cell-mediated liver regeneration via the PTEN-PI3K-AKT-mTOR axis in zebrafish. *Hepatology.* 2021;74(1):397-410.
36. Huang X, Zeng Y, Wang X, et al. FXR blocks the growth of liver cancer cells through inhibiting mTOR-s6 K pathway. *Biochem Biophys Res Commun.* 2016;474(2):351-356.
37. Huang S, Hou Y, Hu M, Hu J, Liu X. Clinical significance and oncogenic function of NR1H4 in clear cell renal cell carcinoma. *BMC Cancer.* 2022;22(1):995.